Robotic Assisted Micromanipulation System using Virtual Fixtures and Metaphors

Mehdi Ammi*, Antoine Ferreira†

*LIMSI-CNRS, Université de Paris Sud, France
Email: mehdi.ammi@limsi.fr
†Laboratoire Vision et Robotique
ENSI de Bourges - Université d'Orléans, France
Email: antoine.ferreira@ensi-bourges.fr

Abstract— This paper describes the use of virtual fixtures and metaphors of assistance for robotic-assisted micromanipulation system in order to prevent the influence of microphysics on path planning and handling tasks. The system is based on a multimodal telemanipulation system using haptic/visual/sound interfaces for observation of microobjects under an optical microscope. Feasible haptically-generated paths based on potentials fields reaction forces and shock absorbers are described for efficient and safe pushing-based or adhesion-based micromanipulation. Then, metaphors with human sensory substitution are proposed in order to improve the perception of data or events. Finally, an experimental investigation carried out by nine trainees proves that the system guides efficiently and safely the operator's gesture. Moreover, user performance on a given task can increase as much as 52% in typical micromanipulation tasks.

I. INTRODUCTION

In microscale manipulation, current telerobotic tasks require that the human performs high-precision, repeatable and safe operations in confined environments. Some examples can be found typically in microelectromechanical (MEMS) assembly systems [1] or in the injection of substances (DNA,RNA) in biological cells [2]. Currently, such tasks are performed under an optical microscope where forces are imperceptible and depth measurement limited. Tremor, fatigue, and stress are magnified which affects the accuracy and efficiency of the micromanipulation tasks. Vision-based virtual fixtures can overcome human limitations by providing guidance and assistance tools to robot-assisted micromanipulation tasks [3],[4]. In the field of micromechatronics, Song *et al.* [5] proposed a telemicromanipulation system assisted by augmented reality. Visual virtual guides are used for enhancing the visibility and perception of the operator performing microassembly tasks. In the domain of biology and surgery, Kumar *et al.* [6] experimented a Steady Hand robotic system (SHR) for vitreoretinal microsurgery where guidance virtual fixtures improved the speed and efficacy of the procedure. Based on the SHR system, Kapoor *et al.* [7] proposed also the use of vision-based virtual fixtures in the force control for safe biological microinjection tasks.

Consequently, this approach overcomes inadequate precision control over motion and force in freehand procedures. The virtual fixtures can restrict motion in given directions and/or planes in order to guide motion towards specific locations [8]. They permit the operator to perform tasks with higher confidence and accuracy with the knowledge that the typical limitations of human skill at the microscale have been largely overcome. Studies have shown that user performance on a given task can increase as much as 70% after the introduction of virtual fixture guidance [9]. Virtual fixtures can be designed to have different levels of motion guidance, ranging from complete free guidance (hard fixture), limited guidance (soft fixture) and no guidance. Generally, most of the micromanipulation tasks requires a mixture of these three types of fixtures. As example, in a microassembly robotic task different fixtures are required following the task decomposition: (i) avoidance of obstacles (no guidance), a path following mode (soft fixture) and an insertion mode (hard fixture) [10]. In this study, several virtual fixtures are proposed, experimented and characterized.

In Section 2, we describe an multimodal human-machine interface based on virtualized reality techniques for real-time telemicromanipulation with vision, force and sound feedback. Then, different virtual fixtures are proposed in Section 3 for operator guidance and assistance during micromanipulation tasks. Finally, Section 4 presents a series of experiments to validate the proposed virtual haptic fixtures.

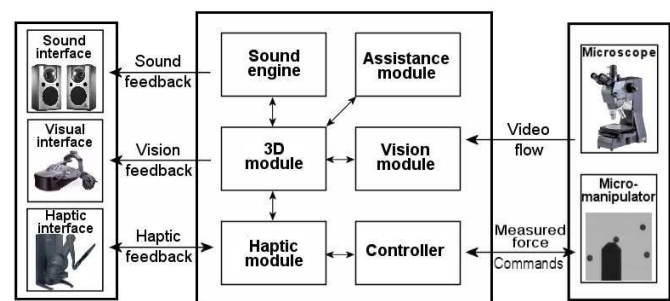## II. MUTISENSORY TELEMICROMANIPULATION SYSTEM

Fig. 1.   Architecture of the multisensory telemicromanipulation system.

Fig.1 shows a multisensory human-machine interface (HMI) system connected to an AFM-based micromanipulator working through the field of view of an optical microscope. In this
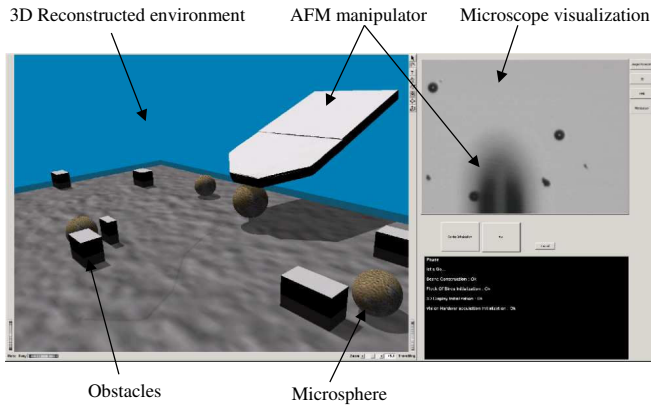
Fig. 2. Graphical user interface (GUI) integrating the real imaging (right side) provided the optical microscope and the reconstructed virtual microenvironment (left side) during real time AFM micromanipulation.
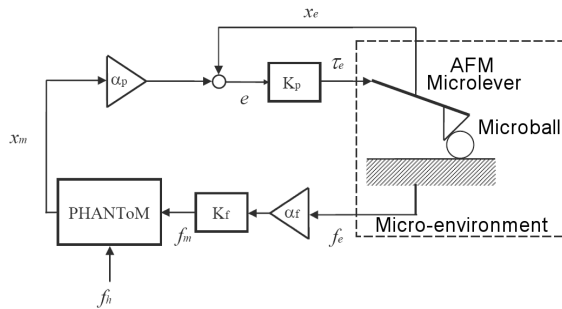

Fig. 3. Bilateral controller for kinesthesic force feedback.

work, it should noticed that the AFM equipment is not used for atomic-scale manipulation nor AFM-scanning mode. The HMI is basically composed of virtual reality input/output devices connected to a virtualized reality interface (Fig.2). The goal of the developed human-machine interface is the improvement of the communication between the operator and the microenvironment through adequate interaction (haptic feedback, vision feedback and sound feedback). The multimodal HMI proposes assistance tools well adapted to the operational context of the micromanipulation tasks such as virtual metaphors, virtual fixtures and potential fields. As shown in Fig.2, the proposed interface is based on the virtualization concept of the microenvironment. It formulates the virtualized reality of the microenvironment through two sources of information (Fig.2): (i) from real image provided by optical microscopy and (ii) from synthetic views generated by a 3D model of the remote microworld. It reconstructs the scene, and manages microobject behaviors in the simulation loop while processing sensor data from the real world (the reader should refer to [11] for further explanations). The operator does not act directly on the real microscene but only on its virtual equivalent ensuring in this way a safe decoupling interface between the teleoperator (active part) and the microenvironment (passive part). The operator gestures are then retransmitted in real-time to the AFM manipulator according to the his manipulation skills.

The micromanipulator structure is composed of three linear translation stages (x,y,z) driven by DC motors for coarse motion (range: 8 mm, accuracy: 15 nm) combined with a 3 d.o.f ultra-high-resolution piezomanipulator (x,y,z) for fine positioning (range: 100 μm, accuracy: 1 nm). This hybrid nanopositioning system combines the advantages of ultra-low inertia, high-speed and long travel range. The endeffector is constituted by a piezoresistive AFM cantilever integrating a full-bridge strain gauge sensors. A kinesthesic force feedback (KFF) bilateral controller allows the operator to feel the microforces sensed by the AMF cantilever (Fig.3). The "ideal" controller response is given as

$$
\begin{aligned}
x_e &\rightarrow \alpha_p x_m \\
f_m &\rightarrow \alpha_f f_e
\end{aligned}
\tag{1}
$$

Here, $\alpha_p > 0$ and $\alpha_f > 0$ are respectively the position and force scaling factor. The bilateral controller is chosen such as

$$
\begin{aligned}
f_m &= \alpha_f\,K_f\,f_e \\
\tau_e &= K_p\,(\,\alpha_p\,x_m\,-\,x_e)
\end{aligned}
\tag{2}
$$

where K_p and K_f are respectively the position and the force compensation gains.

III. VIRTUAL FIXTURES FOR OPERATOR GUIDANCE

Haptic virtual fixtures and more generally virtual metaphors of assistance are an important contribution of virtual reality to the teleoperation-assisted micromanipulation domain. The virtual fixture control mode can be used within two contexts: when providing an alternative to path planners during supervisory control, or when providing a task-dependent aid for manual control during execution in the master/slave mode.

A. Path planning for optimal micromanipulation

In order to optimize the handling during the microsphere displacement, it is necessary to use a virtual guide which generates an optimal trajectory to pass from an initial configuration to a final one. This fixture include functions that allow the operator to take into account the micromanipulator kinematics (limited degrees of freedom, non-holonomic singularities, nature and geometry of tool shape) and the microphysical constraints due to adhesive microforces (van der Waals, electrostatic, surface tension). In the following, we assume as a first approximation that the substrate is smooth. However, the topography of the substrate surface must be carefully analyzed when choosing the optimal path in order to avoid collisions with bumps or substrate defects. The adopted procedure for the microsphere displacement (A) through the field of obstacles (B_i / $i \in 1, ..., n$) includes the following steps :

1) Configuration space obstacles : The following algorithm consists to generate a set of paths in the free space while respecting maximization of the distance from obstacles in order to avoid attraction forces due to microphysics. The configuration space indicates the own space of the microsphere A. The configuration space of A, noted (CS), defines all

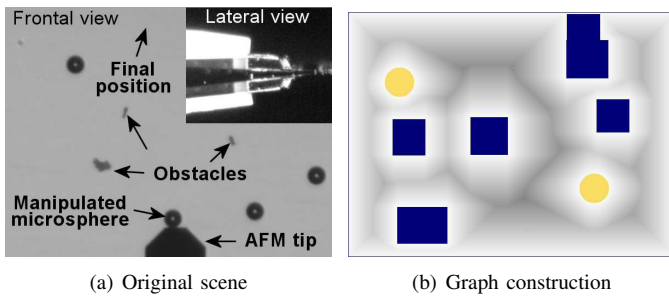(a) Original scene   (b) Graph construction

Fig. 4. Optimal path calculation steps.

possible configurations (positions and orientations) which can be taken by the micromanipulator. CS is composed by two components : 1) $CS - obstacles$ and 2) $CS - free$. The term $CS - obstacles$ indicates the areas of W which are not accessible to A. We defined $A(q)$ the points that can be occupied by the microsphere in the configuration q

$$\text{CS-obstacles}_j \ = \ \{ \ q \ \in \ CS \ / \ A(q) \ \bigcap \ B_j \ \neq \ \emptyset \ \} \tag{3}$$

Generally, this space is determined by the manipulator kinematic constraints. However, we should consider also the constraints induced by the environment microphysics, i.e. van der Waals, electrostatic and surface tension forces. The configuration space obstacles $CS - obstacles$ is calculated by enlarging obstacles with a safe distance (Fig.4(b)). The complement of the $CS - obstacles$ defines a subspace of CS where A is free of any contact. This space defines the free space, termed $CS - free$.

2) Graph construction: It consists to generate a graph that represents all possible trajectory paths. Several methods have been proposed (cell decomposition, visibility graph, probabilistic roadmap, potential field). In our graph construction, we chose the generalized Voronoï diagram (noted GVD) belonging to the roadmap family. Its principle is based on the calculation of a graph of edges that are equidistant from obstacles using a wave front expansion [12]. We start the wave front in each pixel included along the edge of an object, and we labelled each pixel by an unique ID. This ID is given to all direct neighbors. When two different IDs are in collision, we defined the middle between two close objects. Once the GVD is calculated, we connect the handled microsphere center and the target to the GVD by a virtual line (Fig.4(b)).

3) Optimal path calculation: The graph search algorithm is based on a sequence of arranged formations and postures from initial node to final node. Towards this end, we chose the best established algorithm for searching optimal paths, namely "A-star" algorithm [13]. This algorithm is based on the Dijkstra [14] procedure to which an orientation research analysis is added [15]. This heuristic search ranks each node, n, by an estimate of the best route that goes through that node. The typical formula is expressed as:

$$f(n) = g(n) + \mu \ h(n) \tag{4}$$

where
- $f(n)$: is the total estimated cost of the path passing by the node n ;
- $h(n)$: is the estimated cost from the node n to the goal node on the basis of the Manhattan distance ;
- $g(n)$: is the cost from the starting node until the node n ;
- μ : indicates the importance of $h(n)$.

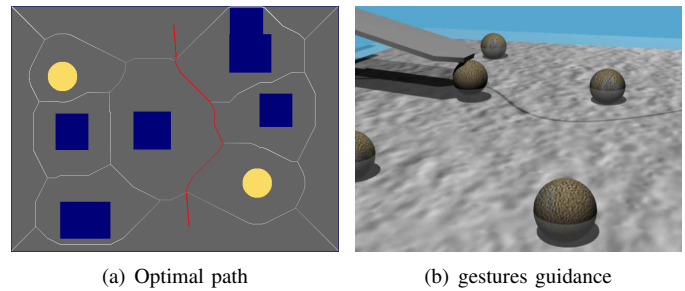(a) Optimal path   (b) gestures guidance

Fig. 5. Operator's gestures guidance.

The "A-star" algorithm explores all routes through the graph that encapsulates the paths connecting nodes together. Since the micromanipulator can only push following piecewise linear paths, the applied algorithms propose ideal moving trajectories for the AFM-based robot. Due to the non-holonomic constraints of the manipulator, configuration space around convex corners are mostly avoided (circular arcs).

4) Operator gesture guidance: Once the shortest path is generated (Fig.5(a)), the path planning module transmits simultaneously the optimal trajectory to the visual and haptic rendering modules. The optimized path determined in the previous section is materialized on the 3-D visual interface as a virtual line between the AFM-based manipulator's tip and its target location for perceptual aid during manual tele-micromanipulation tasks. For the haptic rendering, the virtual fixture is showed as a viscoelastic connection between the master device position (PHANToM interface) and the optimal trajectory (Fig.5(b)). The stiffness K and viscosity B of the mechanical connection must linearizes the operator trajectory while constraining sufficiently its gesture. The values of K and B should be selected appropriately in order to avoid jerked and unstable haptic feedback (at high force-feedback values) or important trajectory errors.

B. Potential fields for safe micromanipulation

During telemicromanipulation tasks, the operator can potentially collide with dust and/or sphere particles which are present in the configuration space. Owing to the dust physical interaction properties attractive forces can greatly disturb the manipulation operations. The solution is to use potential fields as virtual constraints which are implemented in the master's haptic controller (PHAMToM Desktop stylus). The main interest of the proposed method is the real-time obstacle avoidance in path planning since it avoids the use of heavy

detection collision algorithms. According to the nature and the objective of the potential fields, we introduced :

1) Repulsive potential field: To deal with the problem of real-time collision-free path planning, virtual repulsive forces are generated around obstacles from discrete potential fields. The idea of this kind of assistance fixture is to achieve guided motion paths of the AFM tip without touching the obstacles. Its role is to prevent the attraction of microobjects by the AFM tip due to adhesion forces (van der Waals force, electrostatic force, surface tension force). This virtual guide appears as an elastic mechanical impedance created at the contact point between the AFM tip and the geometrical representation of the potential field. The expression of this potential field is expressed as follows (Fig.6(c))

$$U_{obstacle}(d) = \begin{cases} \frac{1}{2}\, \eta\, (\, \frac{1}{d} - \frac{1}{d_0}\,) & if \ d \ \le \ d_0 \\ 0 & if \ d \ > \ d_0 \end{cases} \quad (5)$$

where

- d : is the penetration distance ;
- d_0 : is a positive constant which represents the action distance of the potential ;
- η : is a position scaling factor.

2) Potential field as shock absorber: This potential field surrounds the handled microspheres. Its goal is to attenuate the tremors and the abrupt gestures of the operator during approach and/or contact phases. This potentiel field has a spherical geometry and integrates a viscous element acting as a low-pass filter on the operator's gesture. Its simple geometry possess the advantage of being symmetrical and continuous in 3-D space which minimizes the risks of force jump. The shock absorber potential field is given by

$$U_{sphre}(d) = \begin{cases} \lambda\, \frac{\delta d}{\delta t} & if \ d \ \le \ d_0 \\ 0 & if \ d \ > \ d_0 \end{cases} \quad (6)$$

where

- δ : is the partial derivative ;
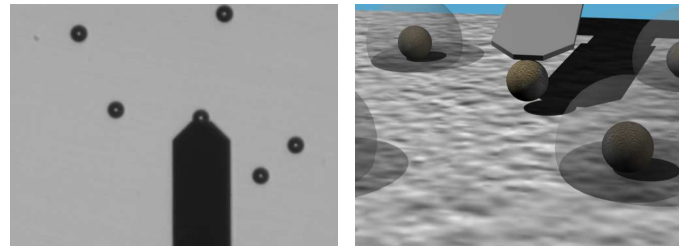- λ : is a position scaling factor.

The global potential field is calculated as the summation of each individual primitive:

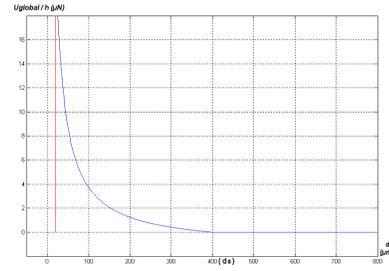$$U_{global}(d) = U_{sphere}(d) + U_{obstacle}(d). \quad (7)$$

The corresponding repulsive force is defined as the negative gradient of potential function, expressed as

$$\overrightarrow{F}(d) = - \bigtriangledown U_{global}(d) \quad (8)$$

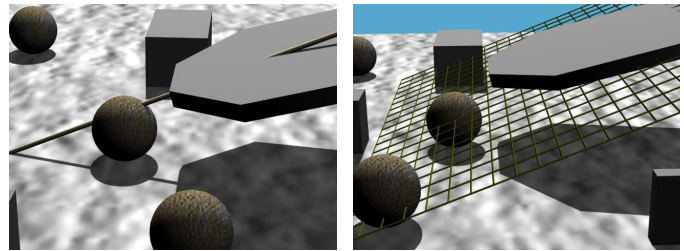where ∇U_{global} represents the Laplacian operator.

(a) Manipulation with potential fields (b) Repulsive potential field representation

(c) Repulsive potential field function

Fig. 6.   The repulsive potential field.

(a) Rectilinear constraint   (b) Plan constraint

Fig. 7.   Gesture constraints.

3) Potential fields as gesture constraints: Haptic virtual fixtures-based guidance strategies are proposed to prevent damage or destruction of microobjects. When the AFM-based micromanipulator is closed to the microobject, visible resolution interaction is not accurate and the AFM tip induces visual occlusion. Furthermore, manipulated objects are not stationary during micromanipulation tasks and the process of locating the objects and repositioning the AFM-tip is not reversible due to thermal effects, drift, hysteresis and nonlinear mechanics. Real-time three-dimensional graphic reconstruction of the real scene was impossible. As illustration, we proposed two virtual guide constraints, i.e. rectilinear (Fig.7(a)) and planar (Fig.7(b)) increasing the performance and safety issues of the operator gesture motions.

IV. METAPHORS WITH SENSORY SUBSTITUTION

Metaphors with human sensory substitution replaces a human sense by another one in order to improve the perception of data or events [15]. The metaphors with sensory substitution move away the virtual action from the real one, nevertheless, immersion and interaction will not be inevitably more difficult to carry out, it requires however more training for a better

assimilation. In our experiments we have exploited the visual and sound modes.

The main objective of the introduction of the sound mode in the proposed multimodal interface is to reduce sensory flow of the visual and haptic channel. Indeed, some informations, as the approach distance or the alarm signals, can easily saturate the operator's perception in the case where information borrows a channel already used for other functions. This effect is accentuated during the critical phases of micromanipulation. Finally, we must notice that virtual guides derived from this mode do not act directly on the operator's gesture but are useful when the intervention requires nonconstrained actions (*passive virtual guide*).

On the basis of the perceptual correspondence between sounds and information [16], we proposed to the operator an auditive representation of the physical data. This metaphor corresponds to an auralisation (symbolic correspondence) of some physical data related to the micromanipulation task :

- The minimum distance between the AFM tip and the manipulated microsphere ;
- The minimum distance between the AFM tip and the optimal trajectory ;
- The force feedback during the interaction with the microenvironment.

These data are represented by a continuous sound proportional to their amplitudes:

- Amplitude modulation ;
- Frequency modulation ;
- Combination of amplitude and frequency modulation.

It should be noticed that the generated sound is in 3-D space in order to allow the estimation of the data direction and the spatial origin of the events. We exploit the binauricular and the monoauricular sound localization cues as follows :

- *Intensity cue* : It is exploited by adding a temporal delay between the right and the left auditive signal according to the direction of variation ;
- *Time cue* : We introduced high frequencies in the auditive signal, variation direction depending on the intensity between both signals ;
- *Phase cue* : This cue is underscored by modulating the high frequency signal by a low frequency signal.

V. EXPERIMENTAL RESULTS

This section presents an experimental investigation carried out on 9 persons with different expertise (experts, students and technicians). The micromanipulation tasks consist to handle several microspheres according to different micromanipulation strategies : 1) micromanipulation by adhesion (spatial displacement strategy) and 2) micromanipulation by pushing (planar displacement strategy). The manipulated microspheres are made of polystyrene with different diameters (*i.e.*, 50.0μm and 20.3μm). In the experiments, we considered the dust particles deposited on the substrate as potential obstacles that should be avoided during micromanipulation tasks.

A. Experimental Setup

The experimental setup shown in Fig. 8(a) is composed of different devices :

- Frontal microscope : A Mitutoyo FS70Z microscope with three objectives;
- CCD camera : A Chugai Boyeki FC-55-II module integrating a Sony sensor with 500-by-582 sensor elements and cell size of 9.8-by-6.3μm ;
- Frame grabber : A mvDELTA Matrix vision frame grabber, with 768-by-576 pixels and pixel frequency of 14.750 MHz ;
- Micromanipulator : A M-111.1 from Polytec PI with an accuracy of 0.05μm and repeatability of 0.1μm with a piezoresistive AFM-tip effector.

For the evaluation of the several immersion, interaction and assistance strategies, we proposed different visual modalities to the operator (Fig.8(b)) such as computer-screen, wide-projection screens (non-immersive mode) or 3-D head-mounted display coupled to a magnetic position tracker (immersive mode). The haptic interaction is carried out via a PHANToM Desktop with 6 dof. Finally, the auditory mode is provided by 3-D sound loudspeaker system for sound spatialization. These different interfaces are shared on three personal computers (pentium IV at 2.8 Ghz). The three units are connected by a local area network (LAN) at 100 Mbps and are organized according to a server/clients architecture.

(a) Micromanipulation setup   (b) Master's part of the telemicromanipulation system
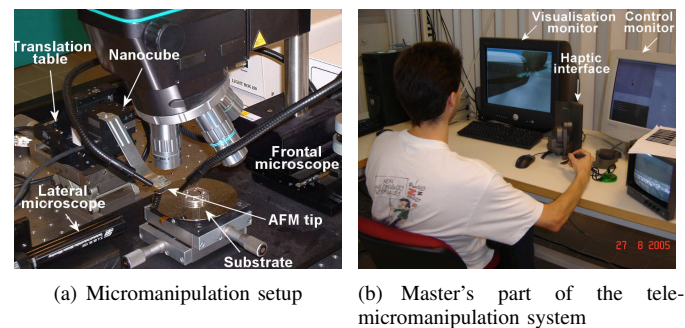
Fig. 8. Human-machine interface.

B. Discussion

In order to demonstrate the advantage of some virtual guides, as well as their impact on the operator's gesture performances, approach and displacement tasks have been tested.

1) Approach phase: The "approach phase" defines a free motion micromanipulation task where the AFM-effector moves from an initial position to a final one until to contact a given microsphere.

Figures 9(a), 9(b) and 9(c) show the velocity of master arm by using several potential field representations. When the operator uses the sound potential field (Fig.9(a)), we observe that after a short period of acceleration, corresponding to the approach phase (effector/potential field), the operator decreases gradually the speed until to reach the contact point.
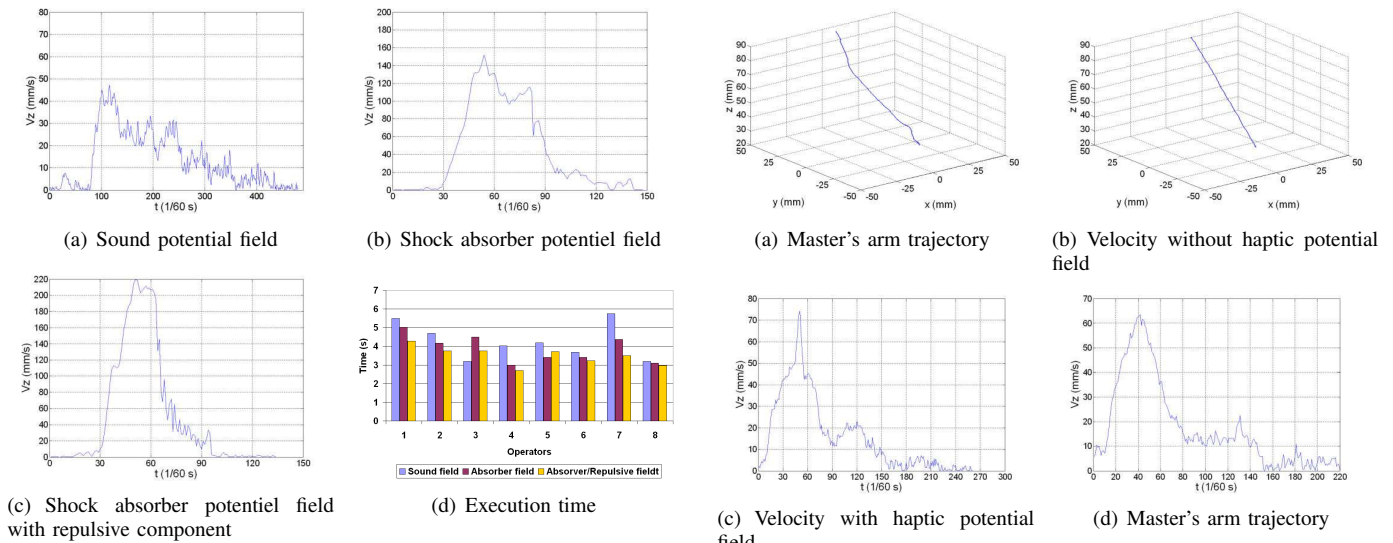
(a) Sound potential field

(b) Shock absorber potentiel field

(c) Shock absorber potentiel field with repulsive component

(d) Execution time

Fig. 9. Velocity and execution time during micromanipulation.

(a) Master's arm trajectory

(b) Velocity without haptic potential field

(c) Velocity with haptic potential field

(d) Master's arm trajectory

(e) Velocity without haptic potential field

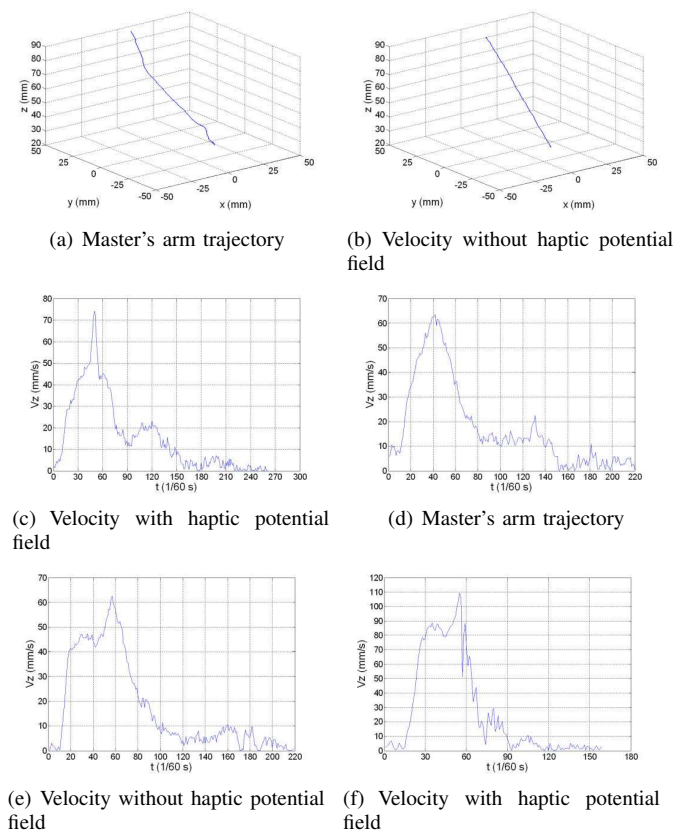(f) Velocity with haptic potential field

Fig. 10. Velocity and trajectory during guided micromanipulation approach for virtual planar motion constraint (figures (a)-(c)-(e)) and virtual rectilinear motion constraint (figures (b)-(d)-(f)).

Fig.9(b) shows that in the case of the shock absorber potential field, the speed values are relatively important (140 mm/s) compared to the a sound potential field representation (50 mm/s). As we can see in Fig.9(d), the execution time is reduced. When we add a repulsive force to a shock absorber potentiel field, the results of Fig.9(b) shows that there is no influence on the behavior of the operator since the operator motion is strongly damped by the virtual guide. The main difference comes from the level of acceleration and speed values during the first phase of the motion (before the contact with the potential field).

In order to reduce tremor and inconsistencies in the free operator motion, some damping and guiding constraints are evaluated through virtual planar and rectilinear guides. As we can see in Fig.10(a) and Fig.10(b), the operator's gesture is more directed without hand tremor in the rectilinear case. We studied also the influence of the operator's gesture velocity (in z-direction) before interacting with a microobject. The results presented in Fig.10(c) and Fig.10(d) show two distinct velocity phases: (i) an acceleration slope in order to closely approach the microsized object and (ii) a deceleration slope followed by a plateau where the operator tries slowly to initiate a contact point by counteracting the adhesive capillary forces. The time of execution is considerably important in both cases. On contrary, Fig.10(e) and Fig.10(f) show better results in terms of execution time and operator's hand velocities when considering haptic potential fields surrounding the microobject. It should be noted in some cases an improvement of 50% in trajectory error and 65% in execution time.

2) Displacement phase: The objective of this experiment is to characterize the combination of different manipulation guides in order to find the optimal fixtures to be adopted for adhesion-based micromanipulation tasks. We assume that the microsphere is initially adhered to the AFM-tip before to initiate the displacement task. In this experiment, the operator

must simply move the micromanipulator end-effector from its initial configuration to the final one by avoiding obstacles located in the microscene.

Fig.11(a) shows the master's arm trajectory when the operator uses only the visual representation of the potential field. In this case, the operator moves the end-effector by avoiding the geometrical contact with the visual representation of the potential field (intuitive visual control). So, the operator corrects regularly the end-effector position in order to avoid the contact with the visual potential fields. When considering potential fields with repulsive force feedback (Fig.11(c)), we noticed that the operator's gesture is controlled in a precise and direct way with less motion readjustments. The velocity curves shown in (Fig.11(b)) and Fig.(11(d)) confirm these first observations. We noticed also that in the case of the visual representation, operator motions are relatively slow with frequent acceleration and deceleration phases. On contrary, haptic feedback improves greatly the operator gesture since he feels less stressed. The velocity achieved in this case is more important, around $v_z \approx 80$ mm/s versus $v_z \approx 30$ mm/s in the previous case.

Finally, Fig.(12(a)) emphasizes the relatively important gain on the execution time. Fig.13 shows the operator trajectories when using the path planning module. A virtual line is drawn
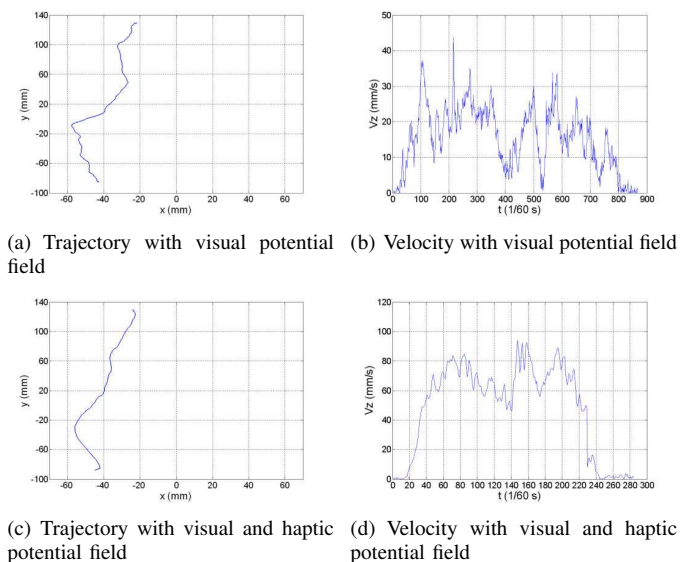
(a) Trajectory with visual potential field

(b) Velocity with visual potential field

(c) Trajectory with visual and haptic potential field

(d) Velocity with visual and haptic potential field

Fig. 11. Master's arm trajectory and velocity with visual and haptic potential field during the microsphere displacement.
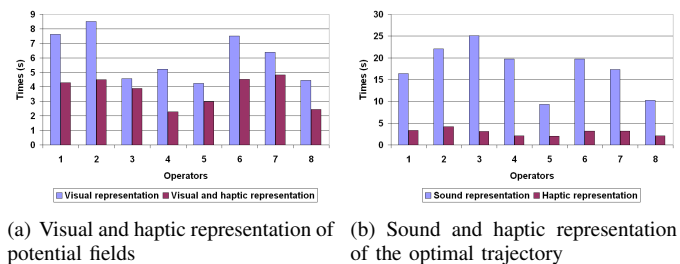

(a) Visual and haptic representation of potential fields

(b) Sound and haptic representation of the optimal trajectory

Fig. 12. Execution time for optimal path and potential field.

(a) Trajectory with sound representation

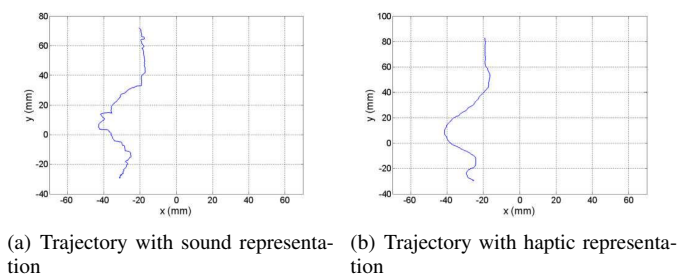(b) Trajectory with haptic representation

Fig. 13. Master's arm trajectory with sound and haptic representation of the optimal trajectory.

between the AFM-tip and its intended target for perceptual aid during manual telemicromanipulation tasks. The Fig. 12(a) represents the trajectory guidance results based on sound feedback. It shows clearly the difficulty encountered by the operator to follow the optimal path. Indeed, the operator readjusts frequently the end-effector's position close to the optimal path with respect to different sound modulations (amplitude, frequency and amplitude/frequency). As it is shown in Fig.13(b), trajectories obtained with haptic constraint are totally smoothed. In later case, the operator gesture is being entirely guided by the haptic virtual guide. These haptically-

generated paths are materialized as the generation of virtual reaction force between master and suggested virtual work path during human operation. Furthermore, the execution time is less important than the sound mode (Fig.12(b)).

VI. CONCLUSION

The teleoperation scheme based on virtual fixtures and metaphors using vision/haptic/aural feedback enables the operator to transfer both motion, vision and human skills at the microscale. The different experiments that have been carried out in this study show clearly the interest of some virtual fixtures for operator guidance and assistance during manual telemicromanipulation tasks. The main advantage is that the operator concentrates only on the useful part of operational gesture, improving in this way the task execution, the execution time and the safety of the micromanipulation task. Furthermore, as the mental effort is reduced it contributes to increase the operator endurance and expertise. A selection of the appropriate level of immersion has been proposed depending on the requirements of the tasks and the usability of the immersion techniques provided to the operator.

REFERENCES

[1] M.Sitti, H.Hashimoto, Two-Dimensional Fine Particle Positioning under an Optical Microscope using a Piezoresistive Cantilever as a Manipulator. *Journal of Micromechatronics*, Vol.1, No.1, pp.25-48, 2000

[2] J. Kuncova-Kallio, P. J. Kallio, Lab Automation in Cultivation of Adherent Cells. *IEEE Transactions on Automation Science and Engineering*, Vol.3, No.2, pp.177-186, April 2006.

[3] A. Bettini, P. Marayong, S. Lang, A. M. Okamura, G. D. Hager, Vision-Assisted Control for Manipulation using Virtual Fixtures, *IEEE Transactions on Robotics*, Vol.20, Issue 6, pp. 953-956, 2004.

[4] J. J. Abbott, P. Marayong and A. M. Okamura, Haptic virtual fixtures for robot-assisted manipulation, *12th International Symposium of Robotics Research*, San Francisco, USA, 2005.

[5] E. Song, D. Kim, K. Kim, J. Lee, Intelligent user interface for tele-operated microassembly, *Int. Conference on Control, Automation and System*, pp.784-788, 2003.

[6] R.Kumar, T. Goradia, A. Barnes, P. Jensen, L. Whitcomb, D. Stoianovici, L. Auer, and R. Taylor. Performance of robotic augmentation in common dexterous surgical motions. *MICCAI*, Vol.1679, pp.1108-1115, 1999.

[7] A. Kapoor, R. Kumar, R. H. Taylor, Preliminary experiments in robot-human cooperative microinjection. *IEEE Int. Conference on Robotics and Automation.*, Las Vegas, 27-31 October, pp. 3186-3191, 2003.

[8] C.A. Sayers. *Remote Control Robotics*. Springer-Verlag, London, 1998.

[9] L. Rosenberg. Virtual Fixtures. PhD thesis, Dept. of Mechanical Engineering, Stanford University, 1994.

[10] M. Hamdi, A. Ferreira, Microassembly Planning using Physical-based Models in Virtual Environment, *IEEE Int. Conference on Robots and Intelligent Systems* , November, Sendai (Japan), pp.3369-3374, 2004.

[11] M. Ammi,A. Ferreira, Virtualized Reality Interfaces for Tele-Micromanipulation, *IEEE Int. Conference on Robotics and Automation*, April 26-May 1, New Orleans LA (USA), 2004.

[12] C. O'Dunlaing and C. Yap, retraction method for planning the motion of a disc, *Journal of Algorithms*, Vol. 6, N 1, 1982.

[13] A. J. Patel, Amit's thoughts on path-finding and A-Star, *http://theory.stanford.edu/ amitp/GameProgramming/index.html*, 2003.

[14] J. C. Latombe, Robot Motion planning, *Kluwer Academic Publishers*, 1991.

[15] M. Kitagawa, D. Dokko, A.M. Okamura and D.D. Yuh, Effect of sensory substitution on suture-manipulation forces for robotic surgical systems. *The Journal of thoracic and cardiovascular surgery* , 2005.

[16] V. Derveer, Ecological acoustics : human perception of environmental sounds, *Dissertation Abstracts International*, Vol. 40/09B, 1979.